Multi-material distributed recycling via Fused granular fabrication: rHDPE and rPET case of study

Catalina Suescun Gonzalez[1,], Hakim Boudaoud[1], Cécile Nouvel[1], Fabio A. Cruz Sanchez, Joshua Pearce[1]

[a] *Université de Lorraine, F-54000, Street Address, City, 54000*

[b] *Western University, Department of Electrical & Computer Engineering, Canada, London, 54000*

Abstract

The high volume of plastic waste and the extremely low recycling rate has created a serious challenge worldwide. Local distributed recycling coupled to additive manufacturing (DRAM) offers a solution by economically incentivizing local recycling. A new DRAM technology capable of processing large quantities of plastic waste quickly is fused granular fabrication (FGF), where solid shredded plastic waste can be reused directly as 3D printing feedstock. This study presents an experimental assessment of multi-material recycling printability, using two of the most common thermoplastics in the beverage industry polyethylene terephthalate (PET) and high-density polyethylene (HDPE) and the feasibility of mixing PET and HDPE to be used as a feedstock material for large-scale 3-D printing. After the material collection, shredding, and cleaning its characterization, and optimization of parameters for 3D printing was performed. Results showed the feasibility of printing a large object from rPET/rHDPE flakes reducing the production cost up to 88%. .

Keywords: keyword1, keyword2

*Corresponding author

1. Introduction

The disposal of plastic waste is one of the most challenging current environmental concerns given its systemic complexity (Evode et al., 2021). The mass of micro- / meso- plastics in the oceans are expected to exceed the mass of the global stock of fish by 2050 (MacArthur, 2017). More critically, the global plastic annual production is expected to reach 1100 metric tons by the same year (Geyer, 2020). The societal awareness on plastic recycling have received substantial attention by scientific, policymaker and general public (Soares et al., 2021). Unfortunately, the statistical analysis on the centralized recycling process proves that it has been largely ineffective (**godswillImpactsPlasticPollution2019a?**) as only 9% of the plastic that has been produced has been recycled from the total stock produced since 1950 (Geyer et al., 2017). Therefore, it remains an open challenge to identify alternatives to valorize discarded plastic material.

Distributed recycling and additive manufacturing (DRAM), is an innovative technical approach to recycle plastic wastes (Cruz Sanchez et al., 2020; Dertinger et al., 2020). DRAM was first practiced with recyclebots, which are waste plastic extruders that made filament for conventional fused filament-based 3-D printers (Baechler et al., 2013; Woern et al., 2018; Zhong and Pearce, 2018). Past research demonstrated that using distributed recycling fits into the circular economy paradigm (Despeisse et al., 2017; Ford and Despeisse, 2016); where consumers directly recycle their own waste into consumer products from open source designs, from toys for children (Petersen et al., 2017) to adaptive aids for those with arthritis (Gallup et al., 2018). Distributed manufacturing is now in wide use (Pearce et al., 2022). In this way DRAM-based recycling is done in a closed loop supply chain network (Santander et al., 2020). This type of recycling aims to reduce the environmental impact by the reduction of the transportation from the waste source to recycling facilities (M. A. Kreiger et al., 2014). In that sense, it aims to propose innovative closed-loop strategies using waste materials as raw resources (Romani et al., 2021).

Fused filament fabrication (FFF, which is also known as Fused Deposition Modelling –

FDM©-) is the most-widespread and established extrusion-based AM technology due to the open source proliferation from the self-replicating rapid prototyper (RepRap) project (Bowyer, 2014; Jones et al., 2011; Sells et al., 2009). This is due to its simplicity, versatility, low-cost, and ability in the construction of geometrically complex objects in the industrial and prosumer domains (**romani2022?**). Indeed, the open-source 3-D approach for 3-D printers has enabled the technology to evolve in a radical manner for manufacturing and prototyping adding value to the recycled material (Cruz Sanchez et al., 2020). There are large efforts to find sustainable feedstocks for 3-D printing (Pakkanen et al., 2017a). Several studies in the literature have increase the spectrum of recycled filament materials such as PLA (Anderson, 2017; Cruz Sanchez et al., 2017a), ABS (Mohammed et al., 2017b, 2017a), PET (Vaucher et al., 2022; Zander et al., 2018), HDPE (Baechler et al., 2013; Chong et al., 2017; Mohammed et al., 2017b) PC (Gaikwad et al., 2018). In fact, using a comparative life cycle assessment in a low density population case study of Michigan, USA, (M. a. Kreiger et al., 2014) argued that about of 100 billion MJ of energy per year could be saved in a distributed approach, for the 984 million pounds of HDPE that are recycled in the U.S. There is thus considerable evidence that DRAM can reduce the energy consumption and greenhouse gases of the manufacturing processes.

Most DRAM studies have been using mono-material for the fabrication of feedstock for FFF. There are, however, several examples of mixed materials including wood waste and recycled plastic (Löschke et al., 2019; Pringle et al., 2018) and textile fibers and recycled plastic (Carrete et al., 2021). Recently, (Zander et al., 2019) reported the manufacturing of composite filament from recycled PET/PP and PS/PP blending through compatibilizer copolymer such as SEBS. Their results revealed the technical printability of polypropylene blend composite filaments from a thermo-mechanical characterization perspective. Increasing the performance window of blending materials by compatibilization which could be a relevant path for recycling plastics in a local level and isolated areas contexts (e.g. during humanitarian crises (Lipsky et al., 2019), supply chain disruptions (Attaran, 2020) and/or isolated off-grid situations using solar-powered 3-D printers (**mohammed2018?**)). Likewise, (Vaucher et al.,

2022) studied the evaluation of the microstructure, mechanical performance, and printing quality of filaments made from rPET and rHDPE varying the wt% of HDPE material from 0 to 10%. They confirmed the increase in the Young's modulus from 1.7 GPa of the pure PET to 2.1 GPa for all the HDPE concentrations. Additionally, the maximum stress of the bends were augmented with high HDPE concentrations. Values were lower than virgin PET filament, yet similar to commercial recycle ones. The addition of rHDPE at higher levels, however, helped to meet the brittle-ductile transition in 15% despite the low interfacial tension of both polymers, allowing the printing of quality parts.

While former studies have proven been successful in FFF, a new approach to DRAM is fused granular fabrication (FGF) or fused particle fabrication (FPF), where the material-extrusion AM systems print directly from pellets, granules, flakes, shred or grinder material (Fontana et al., 2022; Woern et al., 2018). In the context of recycling, this could reduce the number of melt/extrusion cycles that degrade the material needed in the filament fabrication process (Cruz Sanchez et al., 2017b). The FGF technique opens up the potential of use recycle materials as well as print large-scale objects either with a conventional cartesian 3-D printer (Woern et al., 2018), delta 3-D printer (Grassi et al., 2019) or hangprinter (Rattan et al., 2023). Research groups corroborate that plastic waste can be used as feedstock materials for FGF/FPF. (Alexandre et al., 2020) assessed the technical and economical dimensions of virgin and shredded PLA printed in a self-modified FGF machine and compared with FFF. The investigation showed that the use of FGF reduced printing cost, time and its mechanical performance was comparable with the obtained using the traditional FFF technique. Likewise, (Woern et al., 2018) found comparable properties between PLA, ABS, PP, and PET recycled and virgin materials. Later publications demonstrated the technical and economic feasibility through the printing of complex objects validating the possibility of recycle plastic with FGF in both conventional and common FFF materials (Byard et al., 2019), but also recycle PC (Reich et al., 2019) and rPET (Little et al., 2020,). Few researchers, however, have addressed the problem of the direct printing of recycled multi-materials, which might be a key step forward needed to facilitate the ease of sorting and recycling post-consumer

plastic waste materials.

This study explores the potential of direct 3-D printing two immiscible polymers commonly used in the beverage sector through a distributed recycling process for its easily implementation operation at the local level. To demonstrate the feasibility of the process, the bottled water plastic most used in France of roughly 90% of PET (body of the bottle) and 10% of HDPE (cap) now called *rPET90//rHDPE10*, is used as a test material. The experimental process of collection, characterization, and printing of the recycled material is described and the results are discussed in the context of widespread DRAM adoption at the community level.

2. Materials and Methods

The methodology presented in Figure **??** outlines the approach adopted to develop the study. The four stages *Material*, *Material preparation*, *Printing process* and *Evaluation* were thoroughly studied in order to control the major processes steps and the technical characterization methods. In the following subsections, each step is explained.

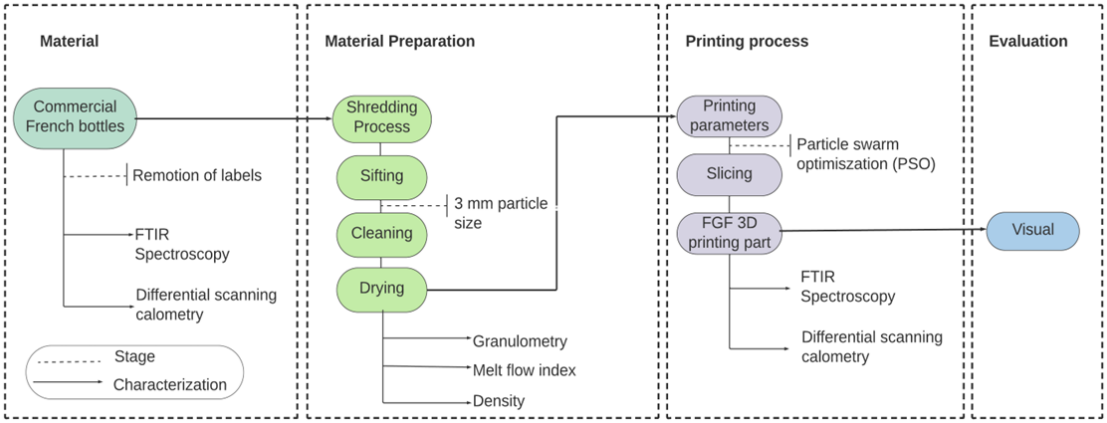

Figure 1: Global framework of the study

2.1. Raw material obtention

The goal of material stage is the collection of post-consumer plastic source. In this study, water of bottles coming from the French brand Cristaline was used as a feedstock. A frame-

work of the process used is shown in Fig. 1.a. Post-consumer bottles were collected by receptacles placed in partnership schools in Lorraine, France. To convert the complete water bottles with its cap into 3DP feedstock material, the labels were removed before shredding in a cutting mill Retsch MS300 using a 3 mm grid. After shredding, the obtained flakes were sifted with a 3 mm sifter. Next, they were cleaned with hot water in an ultrasonic machine at 60°C for 1h to remove contaminants. Lastly, they were dried in a conventional oven overnight at 80°C (Taghavi et al., 2018; Van de Voorde et al., 2022) to avoid degradation of the material. Washing conditions were the same for all the samples, therefore, the effect of contaminants was not considered. The resultant material is shown in Fig. 1.b.

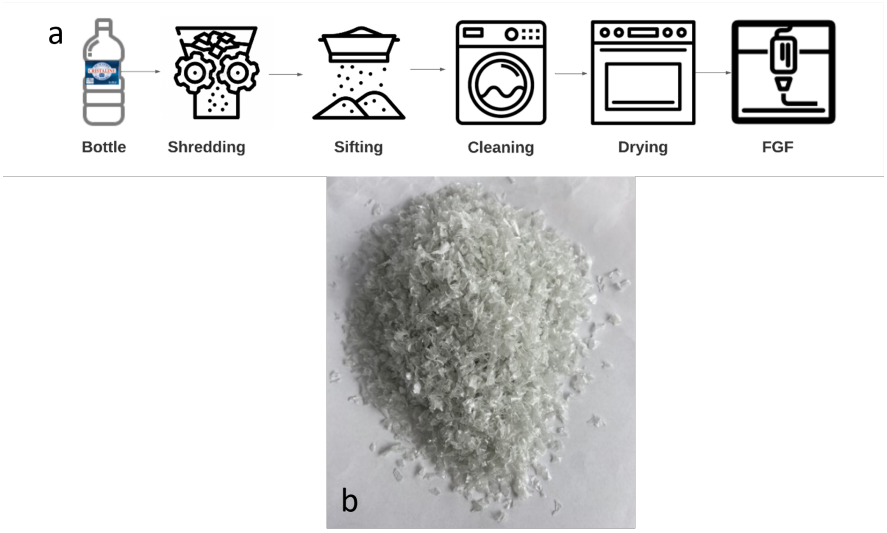

Figure 2: figure1

The material composition was calculated as a function of the mass of the bottles and caps separately. The percent (%) of bottle-cap was found to be ~90%rPET and ~10% rHDPE. The complete bottle was shredded without separation of both materials thus this percentage is constant for all the samples.

2.2. Material preparation

2.2.1. Material particle size analysis -Granulometry-

In order to ensure the particle size suitable for printing, the characterization of the granulate particles were developed using the open-source ImageJ software (**imagej2023?**). The size characteristics of the particles were evaluated between four different samples; vPET (used as a reference) and the raw material sifted in three different sizes 1.5 mm, 3 mm and 5 mm.

2.2.2. Fourier-transform infrared spectroscopy –FTIR-

FTIR spectroscopy was carried out to determine the nature of the bottle and determine if there were impurities, plasticizers or additives that could be detected. The analysis were made on samples of rPET and rHDPE separately and then a printed sample of both materials to determine if there was possible to observe a chemical bonding. Every sample was measured in two different points, three times in each point then curves were normalized and analyzed with the Origin Pro 8 (**https://www.originlab.com/origin?**). The Fourier transform infrared spectra have been recorded in the range of 4000 cm^{-1} to 375 cm^{-1} with resolution 4 cm^{-1} using Bruker IFS 66V spectrophotometer.

2.2.3. Differential scanning calorimetry –DSC-

Differential scanning calorimetry analysis were performed with a DSC-1 Mettler Toledo with STARe software operating under nitrogen atmosphere at heating rate and cooling rate of 10 $°C/min$. rPET, rHDPE and rPET90//rHDPE10 samples were investigated using three cycles: first heating from 20°C to 270 °C, cooling to 20 °C and reheating to 270°C. The rHDPE sample was analyzed following similar cycles but with the maximum temperature set at 250°C and pBC with temperatures from -20 to 270°C. Glass transition temperature (Tg) of rPET was determined during the first heating cycle, while rPET90//rHDPE10 (Tg) during the second heating cycle along with the melting point of all materials. Crystallization temperature (Tc) of the each of the materials was determined during the cooling cycle. The degree of crystallinity (Xc) was calculated from the second cycle for recycled materials and first cycle for the blend as expressed in equation (1) (**aghavi2018a?**; **pan2020?**):

$$X_c(\%) = \frac{\Delta H_m}{w \cdot \Delta H_m^\circ} \tag{1}$$

Where, ΔH_m is the latent heat of melt, w is weight percentage of polymer in the blend, and ΔH_m° is the reference heat of 100% crystalline PET (140 J/g) and HDPE (293 J/g), respectively, provided in the literature (**pan2020?**; **kratofil2006?**).

2.2.4. Melt Flow Index –MFI-

The melt-flow index (MFI) of rPET90//rHDPE10 flakes was determined using a Instron CEAST MF20. The analysis was performed using three samples of ~5 g at 255 °C using a 2.16 kg weight according to ASTM D1238. The process was repeated three times. The average value of the three results was then reported with $gr/10 \times min$ unit.

2.2.5. Density

In order to calculate the material's density, first; the volume was found measuring the dimensions of a solid $50x50x50$ mm cubic geometry fabricated injecting rPET90//rHDPE10 flakes into a square mould with a known volume using open-source desktop injection (Holipress, Holimaker, France) machine. Then the model was weighed, and the mass was obtained. Finally, density was calculated as expressed in Equation **??**. To ensure the accuracy the test was performed twice and the average value was reported in g/cm^3.

$$\rho = V/m \tag{2}$$

Where, ρ is the density, V is the volume, and m the mass.

Afterwards, experimental results were compared with the theoretical blend density which could be calculated by Equation **??**.

$$\rho_{12} = \frac{1}{\frac{W_1}{\rho_2} + \frac{W_2}{\rho_2}} \tag{3}$$

Where, ρ_{12} is the density of the blend, W_1 and W_2, the weight fractions of each polymer, ρ_1 and ρ_2, the theoretical density of each polymer for PET (1.38 g/cm^3) and HDPE 0.93 to 0.97 g/cm^3 (Jonathan GUIDIGO1 et al., 2017).

2.3. Printing process

2.3.1. Establishing optimal parameters

Establishing optimum combinations of parameters is essential for better quality and mechanical properties of the printed parts (Jaisingh Sheoran and Kumar, 2020). According to (Oberloier et al., 2022a), particle swarm optimization (PSO) is an effective and time-effective method for this purpose. The optimization of the 3-D printing parameters for the rPET90//rHDPE10 material in the GigabotX was performed using the open-source PSO Experimenter platform (available in Linux), following the methodology developed by (Oberloier et al., 2022a). Three process benchmark artifacts were printed; line, plane, and cube. They were modeled in CAD software Onshape CAD v1.150 and sliced using Prusaslicer v2.52.0. The geometry models and dimensions are shown in Fig. 2.

Geometry	Lenght (mm)	width (mm)	height (mm)
Line	200	2	1
Plane	100	100	1
Cube	40	40	40

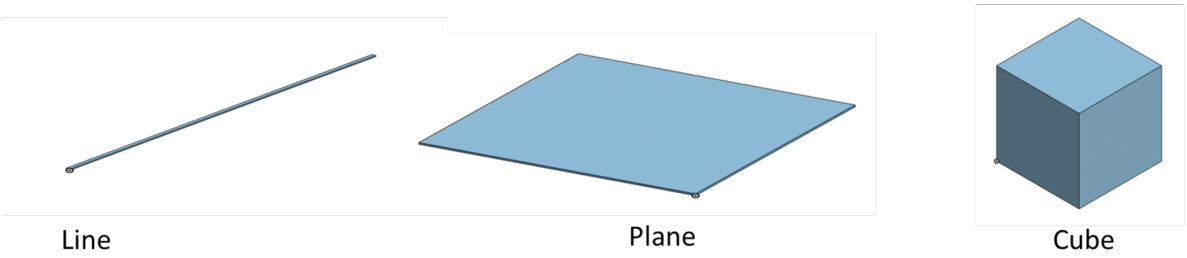

Figure 3: Dimensions and CAD models of the geometries used for parameters optimization.

Four parameters were assessed: 1) the nozlle temperature, 2) bed temperature, 3) the printing speed and 4) extrusion multiplier (Oberloier et al., 2022b). The initial parameters for the line are presented in Table 1.a while other parameters were obtained in preliminary experimental work shown in Table 1.b. Finally, the PSO tuning parameters were found in the previous PSO work (Oberloier et al., 2022a) Table 1.c.